molecule (*9*). However, the molecules are not necessarily sampling all spherically symmetric orientations. It is possible, for example, that in the fcc phase the long axes of the molecules randomly sample the different ⟨111⟩ directions.

Our data indicate that the fcc phase is the equilibrium state of pure C_{70} above 300 K. However, the hcp phase is energetically similar to the fcc phase, and can most likely be nucleated by a number of effects, including solvent, powder-grain surfaces, crystal domain boundaries, and so forth. The fraction of hcp phase can thus be reduced by solvent removal, but further reduction requires prolonged thermal annealing, as observed.

REFERENCES AND NOTES

1. J. E. Fischer *et al.*, *Science* **252**, 1288 (1991).
2. P. A. Heiney *et al.*, *Phys. Rev. Lett.* **66**, 2911 (1991).
3. H. W. Kroto *et al.*, *Nature* **318**, 162 (1985).
4. R. Tycko *et al.*, *J. Phys. Chem.* **95**, 518 (1991).
5. W. I. F. David *et al.*, *Nature* **353**, 147 (1991).
6. R. Sachidanandam and A. B. Harris, *Phys. Rev. Lett.* **67**, 1468 (1991).
7. S. Liu, Y-j. Lu, M. M. Kappes, J. A. Ibers, *Science* **254**, 408 (1991).
8. J. R. D. Copley *et al.*, *Physica B*, in press.
9. R. Taylor *et al.*, *J. Chem. Soc. Chem. Comm.* **20**, 1423 (1990).
10. R. M. Fleming *et al.*, *Phys. Rev.* **B44**, 888 (1991).
11. R. M. Fleming, in *Large Carbon Clusters*, American Chemical Society Symposium Series, in press.
12. J. E. Fischer, P. A. Heiney, D. E. Luzzi, D. E. Cox, in *ibid.* (in press).
13. For the powder XRD measurement on the solvent-prepared sample, the experimental configuration at beamline X7A consisted of a Si(111) channel-cut monochromator set for a wavelength of 1.5435 Å, an ion-chamber to monitor the incident beam intensity, and a 1 mm receiving-slit in front of a Peltier-cooled semiconductor detector. The measurements on the sublimed sample employed a wavelength of 1.2987 Å, and a Ge(220) analyzing crystal was placed before the detector to improve the instrumental resolution and enhance the signal-to-background ratio. For measurements on the annealed sublimed sample, a Ge(111) channel-cut monochromator and Ge(220) analyzing crystal were employed, with a wavelength of 1.2981 Å.
14. G. Van Tendeloo *et al.*, *Europhys. Lett.* **15**, 295 (1991).
15. With the use of a Perkin-Elmer 1600 FTIR with a diffuse reflectance attachment, approximately 0.5 mg of C_{70} was placed on a layer of KBr powder on the sample tray. Five hundred scans at 2 cm^{-1} resolution, referenced against the KBr powder itself, were summed. Bands were seen at 504, 534, 564, 578, 642, 674, 794, 1134, and 1430 ± 1 cm^{-1}.
16. Sadtler Research Labs, Standard IR Spectra, No. 419, Philadelphia, PA (1962).
17. D. S. Bethune *et al.*, *Chem. Phys. Lett.* **179**, 181 (1991).
18. Sadtler Research Labs, No. 678, see (*16*).
19. Our estimate of a 0.1% upper limit on the toluene mass can be justified as follows: TGA analysis of vacuum-dried samples shows a weight loss of 3 to 5% in the range 395 to 444 K due to toluene evolution. By comparing the area under the 694 and 724 cm^{-1} IR toluene peaks, we estimate that the sublimed sample has 50 times less toluene than the vacuum-dried sample. The diffuse IR reflectance measurement actually provides the most sensitive measurement of the amount of residual solvent in the sample, since the NMR limit of detectability of residual impurities is generally also in the 0.1% range and often closer to 1 to 2%.
20. Note that the fcc-only peaks are sufficiently weak that they would not have been observed in the spectrum of the solvent-prepared sample, which had a much higher relative level of diffuse scattering.
21. D. E. Luzzi *et al.*, *J. Mat. Res.*, in press.
22. J. Baker *et al.*, *Chem. Phys. Lett.* **184**, 182 (1991).
23. B. E. Warren, *Phys. Rev.* **59**, 693 (1941).
24. We note, therefore, that diffraction patterns collected from such samples at room temperature will generally contain peaks from two or more phases, depending on the thermal history of the sample.

25. We thank A. Denenstein, N. C. Maliszewskyj, P. Sprengler, O. Zhou, and Q. Zhu for their technical assistance, and A. Cheng for useful discussions. This work was supported by the National Science Foundation, under Grants DMR-88-19885 and DMR-89-01219, and by the Department of Energy, DE-FC02-86ER45254 and DE-FG05-90ER75596. The work at Brookhaven was also supported by DOE, Division of Materials Sciences, DEAC02-76CH00016.

3 October 1991; accepted 30 October 1991

Computer Simulations of Self-Assembled Membranes

J.-M. DROUFFE, A. C. MAGGS, S. LEIBLER*

Molecular dynamics simulations in three dimensions of particles that self-assemble to form two-dimensional, membrane-like objects are presented. Anisotropic, multibody forces, chosen so as to mimic real interactions between amphiphilic molecules, generate a finite rigidity and compressibility of the assembled membranes, as well as a finite line tension at their free edges. This model and its generalizations can be used to study a large class of phenomena taking place in fluctuating membranes. For instance, both fluid and solid-like phases, separated by a phase transition, are obtained and some of the large-scale properties of these membranes studied. In particular, thermal undulations of quasi-spherical fluid vesicles are analyzed, in a manner similar to recent experiments in lipid systems.

AMPHIPHILIC MOLECULES THAT ARE brought into contact with water tend to assemble so as to orient their polar hydrophilic "heads" toward the water and their oily hydrophobic "tails" away from it. Among the simplest structures formed in this way are bilayer membranes, whose lateral dimensions can largely exceed their typical thicknesses (*1*). Such (quasi–)two-dimensional molecular assemblies can then form a large variety of thermodynamic phases: closed vesicles, lamellar or cubic crystals, and disordered bicontinuous networks (*2*). Despite definite progress made recently in experimental and theoretical studies of the physical properties of membranes and of the process of their self-assembling (*3*), many aspects of these structures still remain poorly understood. From the theoretical point of view, available analytical and numerical methods are largely insufficient to solve models based on realistic microscopic interactions between amphiphilic molecules surrounded by water. For instance, numerical simulations of truly microscopic models are only possible for very small aggregates such as micelles (*4*). The time scales involved in the largest molecular simulations are much too short to describe the formation and the thermodynamic behavior of larger assemblies such as membranes.

J.-M. Drouffe and S. Leibler, Service de Physique Théorique de Saclay, F-91191 Gif-sur-Yvette Cedex, France. A. C. Maggs, Laboratoire de Physico-Chimie Théorique, Ecole Supérieure de Physique et de Chimie Industrielles, F-75231 Paris Cedex 05, France.

*To whom correspondence should be addressed.

This situation has led to the development of phenomenological theories in which membranes are treated as fluctuating surfaces, described by an effective elastic (free) energy functional, $\mathcal{F}$ (*1*). The effective energy depends on details of shape (such as curvature) (*5*) and topology of the membrane, but it can also take into account additional internal degrees of freedom of its molecular components describing membrane fluidity, chirality, and so forth. Starting with appropriate effective functionals $\mathcal{F}$, one can build thermodynamic models of various types of fluctuating membranes: fluid (*5*), hexatic (*6, 7*), solid-like or polymerized (*6*), with different topologies (*8*) and effective interactions. Because universal properties of the fluctuating membranes (such as the spectrum of their large-scale excitations or the critical indices of various phase transitions involving membranes) should not depend on microscopic details, studying these phenomenological models can yield useful predictions about real systems (*9*).

In this report we describe another approach to the computer simulations of fluctuating membranes. It is similar in spirit to the approach used in many recent numerical studies of solid-like (*10*) and fluid (*11, 12*) membranes in that it does not start with realistic microscopic interactions and thus concentrates only on the universal, large-scale properties of simulated systems. However, in contrast to the previous simulations which start with some kind of a triangulated surface [such as a "tethered" network of impenetrable spheres (*13*) or a surface with fluctuating triangulation (*11*)], the mem-

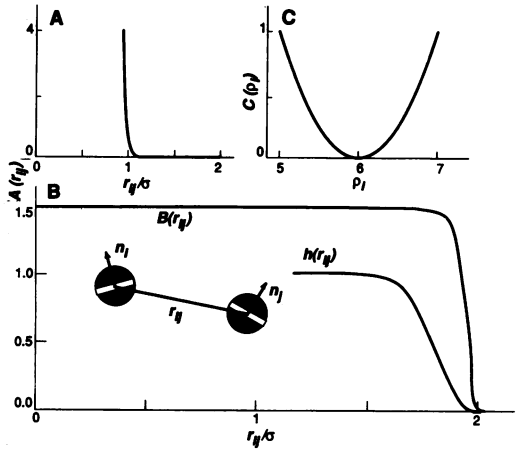

Fig. 1. The interactions between the particles used in the simulation have three distinct contributions. (**A**) A hard core repulsive interaction $A(r_{ij})$, of range σ, ensuring the incompressibility of the molecules at high density. (**B**) An anisotropic interaction, between pairs of particles i and j, of the form $B(r_{ij})\{(\mathbf{n}_i \cdot \mathbf{n}_j)^\alpha + g[(\mathbf{n}_i \cdot \hat{\mathbf{r}}_{ij})^2] + g[(\mathbf{n}_j \cdot \hat{\mathbf{r}}_{ij})]^2\}$ with $\mathbf{n}_i$ and $\mathbf{n}_j$ unit vectors expressing the orientation of the particles and $\hat{\mathbf{r}}_{ij}$ the unit vector between the particles; $g(x) = ax^3 + bx + c$ (in the simulations described below we use a = 0.75, b = 0.25, and c = 0.8); $\alpha = 1$ corresponds to particles with two distinct sides, whereas for $\alpha = 2$ the particles are completely symmetric and $\mathbf{n}_i$ could be replaced by a director. The radial function $B(r)$ smoothly cuts off the interaction for large separations between the molecules. The anisotropic torque from this interaction strongly favors planar configurations of aligned molecules. As a consequence, the particles assemble into a two-dimensional object with a layered structure: the vectors $\mathbf{n}$ can be viewed as being perpendicular to the imaginary "hydrophobic and hydrophilic layers" on each particle (see inset). (**C**) A multibody "hydrophobic" potential that expresses the large increase in free energy occurring when water is in contact with the hydrocarbon parts of the amphiphiles. The entry of the solvent into the membrane is associated with a local depression in the mean density of the amphiphiles. We therefore write this term as a sum $\Sigma_i C(\rho_i)$, where ρ_i is the local density: $\rho_i = \Sigma_j h(r_{ij})$, with $h(r)$ a weighting function. The "hydrophobic" multibody potential is essential for the existence of a two-dimensional fluid phase; without it the particles would evaporate easily from the membrane. All the potentials are measured in terms of an energy scale ϵ.

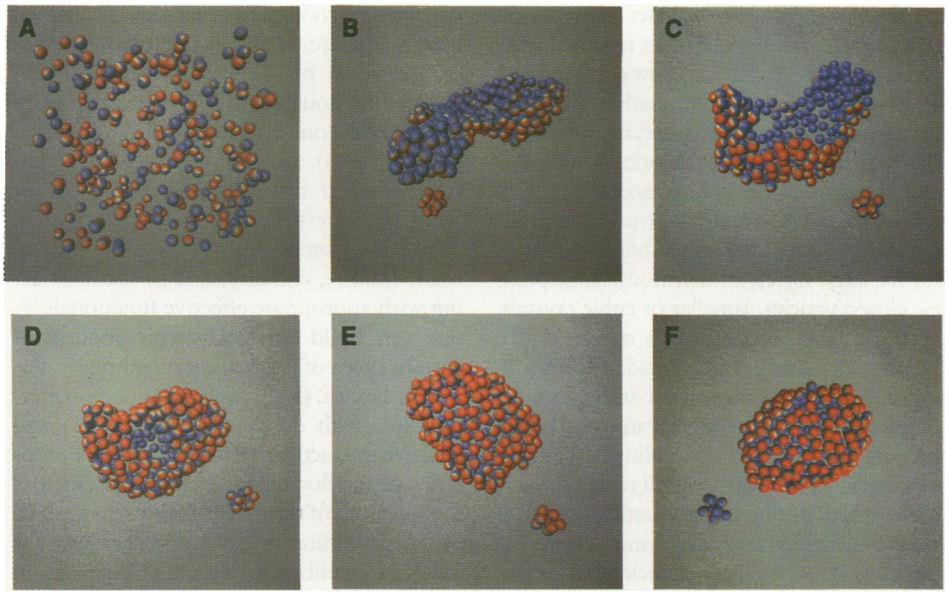

Fig. 2. Evolution in time of an arbitrary random initial distribution of 252 particles enclosed in a box with sides of length 40σ. We made the simulation using molecular dynamics in the presence of weak damping and thermal noise, which permit equilibration at a given imposed temperature (of 1.6ϵ, inside the fluid phase); these correspond to the thermal noise and friction from the solvent present in real system (*16*). Kinematically the particles are taken to be solid spheres of mass m and moment of inertia $2m\sigma^2/5$. The interparticle potentials (Fig. 1) were parametrized by cubic splines, which permit the efficient calculation of the energies and forces acting on each particle. The rotational degrees of freedom were described in terms of quaternions rather than more usual Euler angles (this eliminates the need to calculate trigonometric functions in the equations of motion) (*23*). Each step of simulation consists of integrating the deterministic equations of motion and then thermalizing linear and angular velocities by the addition of small random components. In the initial stage the particles aggregate to form a number of independent segments, which then amalgamate to give one large membrane. (Note, however, the possibility of the formation of several closed vesicles or even small clusters like the one shown on these snapshots.) A finite activation barrier for passing from a nearly flat membrane to a quasi-spherical vesicle results from a competition between the bending energy and the line tension of the edge. After some time thermal fluctuations drive the membrane over this barrier and the vesicle closes. The interaction between the particles does not generate a spontaneous curvature term. Because $\alpha = 1$ here, the particles cluster with well-defined orientations (corresponding to well-separated colors); however, self-assembling of completely symmetric particles ($\alpha = 2$) into the closed vesicles has also been observed. The images are taken at times (**A**) 0, (**B**) $1450t_0$, (**C**) $1920t_0$, (**D**) $2030t_0$, and (**E** and **F**) $2150t_0$, where $t_0 = \sqrt{(\sigma^2/m\epsilon)}$. The influence of the enclosing box is clearly seen in (A).

branes are formed here from interacting particles through a self-assembling process. This approach, somewhat similar to recent simulations of small surfactant assemblies such as micelles (*14*), allows one to study membranes that not only can change their shape but also can vary their internal structure and topology. For instance, self-assembled closed vesicles can exhibit large pores or can even open completely, they can fuse with one another or break into smaller pieces, they can be fluid or can solidify under cooling, and so on.

In order to obtain self-assembling membranes, one has to mimic somehow complex interactions between amphiphilic molecules in water. In our model, interacting particles are hard spheres that can be viewed as consisting of three parts (Fig. 1): a "hydrophobic layer" surrounded by two "hydrophilic layers." The anisotropic attraction between particles is chosen so that the particles aggregate together in such a way that the hydrophobic parts are next to one another. The attraction is short-range and can be described in terms of unit vectors $\mathbf{n}$ associated with each particle and perpendicular to the "layers." (If the membrane is symmetric, the interactions depend only on the direction of $\mathbf{n}$ and not on its orientation; thus $\mathbf{n}$ can be viewed as a director and not a vector.) The two terms, the hard-core repulsion between spheres and the anisotropic attraction, are sufficient to assemble a two-dimensional membrane at low temperatures and give it a finite effective rigidity and compressibility, whose relative values can be varied by changing the amplitudes of these terms. However, in order to have a stable membrane at higher temperatures, that is, a stable quasi–two-dimensional fluid phase with a sufficiently low partial pressure so that vaporization is negligible, one needs to introduce additional interactions. In real phospholipid membranes single amphiphilic molecules cannot leave their neighbors for the solvent because of the large free energy cost of solubilizing their hydrocarbon chains in water. To mimic this "hydrophobic effect" (*15*), we introduce an effective multibody interaction that favors a close-packed environment for each particle (six nearest neighbors); thus it is more difficult for small clusters of particles to leave the fluctuating membrane. With the inclusion of this additional term, membranes are stable well above the melting transition.

We have performed molecular dynamics simulations of N such interacting particles enclosed in a box (*16*), N ranging from 252 to 1962 (Fig. 2). It is a nice feature of the model that, with an appropriate choice of the relative amplitude of the multibody

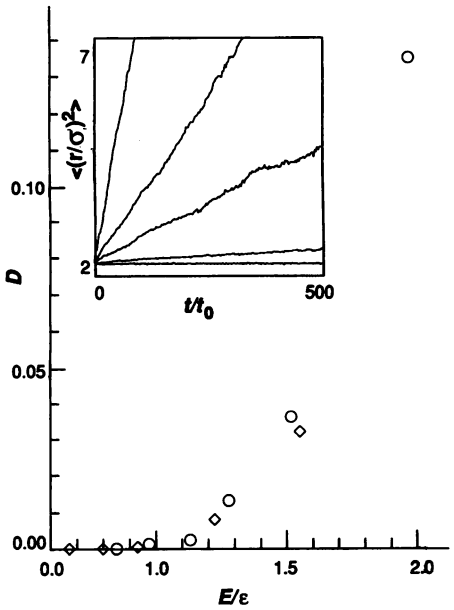

Fig. 3. As the temperature is varied, there is a phase transition from a low-temperature solid phase characterized by very low diffusion constants to a higher temperature fluid phase with much greater molecular mobilities. This transition can be characterized by measuring the diffusion coefficients of the two phases. We have measured the mean squared separation (in three-dimensional space) of two initially neighboring particles as a function of time. The inset contains typical results for different temperatures. At low temperatures the diffusion is so small that initially neighboring particles never separate during the simulation. At higher temperatures the slope of the curve of mean squared separation as a function of time gives a finite diffusion constant. The main figure is a plot of the diffusion coefficient as a function of the temperature (◇, 252 particles; ○, 492 particles). The transition between the low- and high-mobility phases occurs for a value of the mean kinetic energy of about 1.1ϵ.

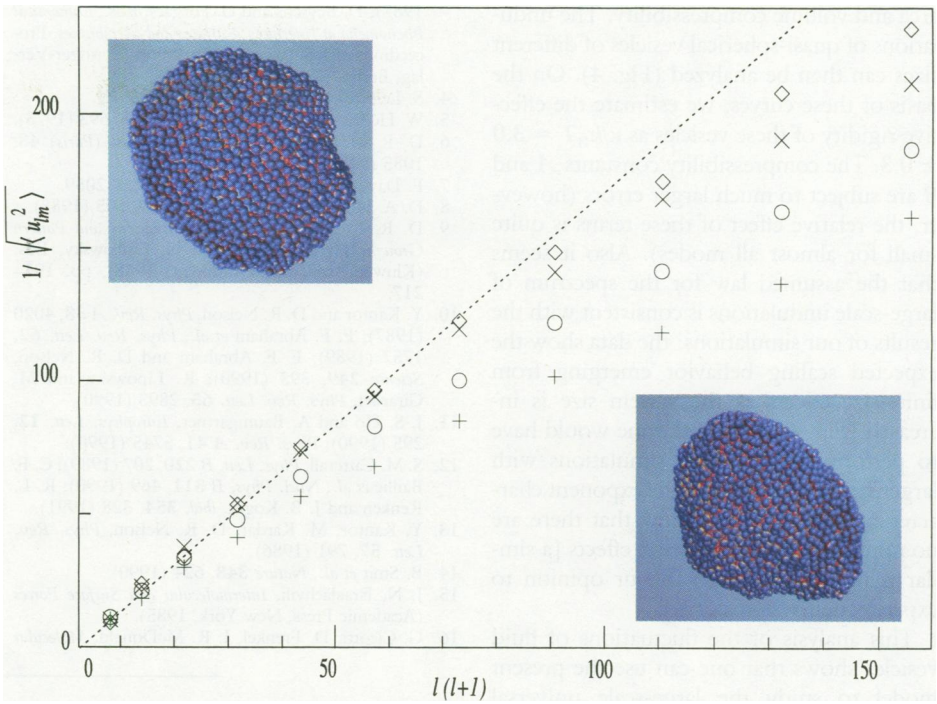

Fig. 4. In the fluid phase, motivated by experiments on quasi-spherical vesicles, we have made a detailed analysis of shape fluctuations. For each vesicle analyzed we first perform a triangulation of the vesicle by going to the center of mass and projecting the particle positions onto a reference sphere of radius R_0. The triangulation is performed by successively adding links between neighbors (sorted in order of their length) until the surface is closed. The shape of the triangulated surface is then expressed as a series in spherical harmonics (Eq. 1). For a surface whose configurations are determined by bending elasticity one expects that $\langle u^2_{\ell m}\rangle = k_B T/\kappa[\ell(\ell+1)]^2$. We have performed simulations for the temperature $k_B T = 1.5\epsilon$ for systems of 252 (+), 492 (○), 1002 (×), and 1962 (◇) particles. A fit to this law (dashed line) allows us to estimate that $\kappa/k_B T \approx 3.0 \pm 0.3$. The insets show two typical configurations of 1962 particles. The simulation time for these systems is $5000t_0$, sufficient for equilibration of $\langle u^2_{\ell m}\rangle$ for all ℓ and m. For 252 and 492 particles this time is also long compared with the time necessary to diffuse a distance R_0; the time for equilibration of the shape fluctuations is short compared to the time necessary to diffuse this distance. For 1962 particles this corresponds to 14 days of calculation on a SUN SPARC1 workstation.

term, an effective line tension generated at the edges of the assembled sheet forces the membrane to close. The closed fluid vesicle fluctuates in shape, and its diffusing particles give rise to finite density fluctuations in the plane of the membrane.

The diffusion of particles forming the membrane can be analyzed quantitatively. The inset of Fig. 3 shows that the time evolution of relative distance of two particles obeys a simple diffusion law. The diffusion constant, D, is practically zero (exponentially small) below some finite temperature T_c, and it increases quickly above T_c (Fig. 3). This temperature corresponds to the melting of membrane and is dependent on the amplitude of different interaction terms as well as on the vesicle size N.

It is important to stress that at low temperatures at which the particles are in solid-like phase and do not diffuse within the plane, the membrane still shows large undulations. The effective rigidity, although higher than that of the fluid phase, is still quite low. In real phospholipid membranes, by comparison, the effective rigidity increases thousands of times below the so-called main transition (*1*). One could take into account this effect, which is due to the ordering of the hydrocarbon chains in solid-like membranes, by introducing an additional term describing the chain degrees of freedom and their coupling to the particle positions and orientations.

We have also analyzed the fluctuations of large quasi-spherical fluid vesicles. This analysis was strongly inspired by a series of recent experiments, made with large phospholipid vesicles (*17*). In such experiments one observes fluctuations of closed fluid membranes under a light microscope and then analyzes the computer-enhanced images containing the shapes of vesicles' contours. As a result, one can extract the values of the rigidity constant, κ, of the membranes and verify the consistency of the observed spectrum of large-scale undulations with the q^4 law (where q is the wave vector of the undulation) (*18*).

One can extend the analytical expressions used to describe the undulations of phospholipid vesicles in terms of spherical harmonics (*19*) to the situation relevant for our simulations, namely, completely permeable membranes (volume fluctuations), with finite density fluctuations (total area fluctuations). Let the shape of a quasi-spherical vesicle be described as a series in spherical harmonics (Fig. 4):

$$r(\theta, \phi) = R_0[1 + \Sigma_{\ell,m} u_{\ell m} Y_{\ell m}(\theta, \phi)] \quad (1)$$

where $r(\theta, \phi)$ is the distance between the center of mass of the surface and the point on the surface with spherical coordinates θ, ϕ, and R_0 is the radius of the reference sphere. If we use the simple q^4 law for the energy of undulations and neglect anharmonic effects, we obtain a general formula for the amplitude of thermally excited undulations $u_{\ell m}$:

$$\frac{1}{\langle u^2_{\ell m}\rangle} = \frac{\kappa}{k_B T}\ell^2(\ell+1)^2 + A\ell(\ell+1) + B \quad (2)$$

where k_B is the Boltzmann constant, T is temperature, and A and B are constants, which in our model are connected with the

area and volume compressibility. The undulations of quasi-spherical vesicles of different sizes can then be analyzed (Fig. 4). On the basis of these curves, we estimate the effective rigidity of these vesicles as $\kappa/k_BT \approx 3.0 \pm 0.3$. The compressibility constants A and B are subject to much larger errors (however, the relative effect of these terms is quite small for almost all modes). Also it seems that the assumed law for the spectrum of large-scale undulations is consistent with the results of our simulations: the data show the expected scaling behavior emerging from finite-size effects as the system size is increased (Fig. 4). However, one would have to perform much longer simulations with larger systems to measure the exponent characterizing this law and show that there are no nontrivial renormalization effects [a similar remark applies also in our opinion to experimental systems (*17*)].

This analysis of the fluctuations of fluid vesicles shows that one can use the present model to study the large-scale universal properties of different types of membranes. It would be interesting, for instance, to search for a "crumpling" transition that has been observed in recent simulations of fluid-like membranes (*12*), a result that seems to contradict other simulations (*11*) or our intuition based on analytical calculations (*18*).

Studies of the large-scale behavior of fluid or solid-like vesicles are among the many possible phenomena that can be considered within the framework of the present model or its generalizations. For instance, we have constructed and have begun to study a structure consisting of a polymerized network attached below a fluid vesicle. Such a composite membrane can be a model for the membranes of red blood cells, in which amphiphilic fluid bilayers are coupled to spectrin cytoskeletons (*20*). Even more interesting should be studies of phenomena that involve changes in membrane topology, such as exo- and endocytosis (*21*). Another simple but spectacular example of topology changes is the recently observed behavior of fluid vesicles made of chiral phospholipids. When such vesicles are cooled below the fluid-solid transition, they break and form helical ribbons (*22*). We believe that the numerical studies of such phenomena could shed light on the general principles of self-assembly in membranes and other molecular systems.

REFERENCES AND NOTES

1. D. R. Nelson, T. Piran, S. Weinberg, Eds., *Statistical Mechanics of Membranes and Surfaces* (World Scientific, Singapore, 1989).
2. For recent reviews, see S. Leibler, *Phys. Rep.* **184**, 265 (1989); R. Lipowsky, *Nature* **349**, 475 (1991).
3. J. Meunier, D. Langevin, N. Boccara, Eds., *Physics of Amphiphilic Layers* (Springer-Verlag, Berlin, 1987); D. Beysens and G. Forgacs, Eds., *Dynamical Phenomena at Interfaces, Surfaces and Membranes*, Proceedings of Les Houches Workshop (Springer-Verlag, Berlin, in press).
4. S. Leibler, *Nature* **348**, 586 (1990).
5. W. Helfrich, *Z. Naturforsch. Teil C* **28**, 693 (1973).
6. D. R. Nelson and L. Peliti, *J. Phys. (Paris)* **48**, 1085 (1987).
7. F. David, E. Guitter, L. Peliti, *ibid.*, p. 2059.
8. D. A. Huse and S. Leibler, *ibid.* **49**, 605 (1988).
9. D. R. Nelson, in *Random Fluctuations and Pattern Growth*, H. E. Stanley and N. Ostrowsky, Eds. (Kluwer Academic, Dordrecht, 1988), pp. 193–217.
10. Y. Kantor and D. R. Nelson, *Phys. Rev. A* **38**, 4020 (1987); F. F. Abraham *et al.*, *Phys. Rev. Lett.* **62**, 1757 (1989); F. F. Abraham and D. R. Nelson, *Science* **249**, 393 (1990); R. Lipowsky and M. Girardet, *Phys. Rev. Lett.* **65**, 2893 (1990).
11. J.-S. Ho and A. Baumgärtner, *Europhys. Lett.* **12**, 295 (1990); *Phys. Rev. A* **41**, 5745 (1990).
12. S. M. Catterall, *Phys. Lett. B* **220**, 207 (1989); C. F. Baillie *et al.*, *Nucl. Phys. B* **311**, 469 (1990); R. L. Renken and J. B. Kogut, *ibid.* **354**, 328 (1991).
13. Y. Kantor, M. Kardar, D. R. Nelson, *Phys. Rev. Lett.* **57**, 791 (1986).
14. B. Smit *et al.*, *Nature* **348**, 624 (1990).
15. J. N. Israelachvili, *Intermolecular and Surface Forces* (Academic Press, New York, 1985).
16. G. Cicotti, D. Frenkel, I. R. McDonald, *Molecular Dynamics and Monte Carlo Methods: Statistical Mechanics of Liquids and Solids* (North Holland, New York, 1987).
17. M. B. Schneider *et al.*, *J. Phys. (Paris)* **45**, 1457 (1984); H. Engelhardt *et al.*, *ibid.* **46**, L395 (1985); I. Bivas *et al.*, *ibid.* **48**, 855 (1987); J. F. Faucon *et al.*, *ibid.* **50**, 2389 (1989).
18. This q^4 law is a simple consequence of the fact that the effective elastic free energy density of the undulating membrane is dominated by the curvature energy term proportional to H^2, where H is the local mean curvature. In harmonic approximation H behaves like the Laplacian operator, thus for small q vectors, like q^2. If one takes into account anharmonic terms, this simple law is modified by logarithmic corrections [W. Helfrich, *J. Phys. (Paris)* **46**, 1263 (1985); L. Peliti and S. Leibler, *Phys. Rev. Lett.* **54**, 1690 (1985)].
19. S. Milner and S. A. Safran, *Phys. Rev. A* **36**, 4371 (1987).
20. B. T. Stokke *et al.*, *Eur. Biophys. J.* **13**, 203 (1986); *ibid.*, p. 219.
21. B. Alberts *et al.*, *Molecular Biology of the Cell* (Garland, New York, 1989).
22. W. Helfrich and J. Prost, *Phys. Rev. A* **38**, 3065 (1988).
23. D. J. Evans and S. Murad, *Mol. Phys.* **34**, 327 (1977).

6 June 1991; accepted 8 August 1991

Major Role of the Cyanobacterium *Trichodesmium* in Nutrient Cycling in the North Atlantic Ocean

EDWARD J. CARPENTER* AND KRISTEN ROMANS

The diazotrophic cyanobacterium *Trichodesmium* is a large (about 0.5 by 3 millimeters) phytoplankter that is common in tropical open-ocean waters. Measurements of abundance, plus a review of earlier observations, indicate that it, rather than the picophytoplankton, is the most important primary producer (about 165 milligrams of carbon per square meter per day) in the tropical North Atlantic Ocean. Furthermore, nitrogen fixation by *Trichodesmium* introduces the largest fraction of new nitrogen to the euphotic zone, approximately 30 milligrams of nitrogen per square meter per day, a value exceeding the estimated flux of nitrate across the thermocline. Inclusion of this organism, plus the abundant diazotrophic endosymbiont *Richelia intracellularis* that is present in some large diatoms, in biogeochemical studies of carbon and nitrogen may help explain the disparity between various methods of measuring productivity in the oligotrophic ocean. Carbon and nitrogen fixation by these large phytoplankters also introduces a new paradigm in the biogeochemistry of these elements in the sea.

IT IS NOW COMMONLY ACCEPTED THAT picophytoplankton (<2 μm) are the major primary producers and constitute the largest fraction of the standing crop of phytoplankton in oligotrophic marine waters; this implies that large phytoplankton play a minor role in carbon and nitrogen cycling (*1–4*). However, because of sampling inadequacies, the very large (~1 to 3 mm) phytoplankton such as the diazotrophic (nitrogen fixing) cyanobacterium *Trichodesmium* have been underrepresented in most oceanic biomass and C and N flux measurements. A reevaluation of past studies on phytoplankton species distribution, and recent measurements, indicate that *Trichodesmium* is usually the most important phytoplankter as regards standing crop and productivity, and, through N_2 fixation, is the major source of new N to the euphotic zone of the tropical North Atlantic Ocean.

In the equatorial Atlantic Ocean, the less than 1-μm size class has been reported to contain an average of 44 to 71% of the total chlorophyll *a* (chl *a*) (*2, 4*), and to be responsible for 60% of the primary productivity (*4*). Similar observations have been made for the tropical Pacific Ocean (*3*). The discovery of this prokaryotic (*5, 6*) and eukaryotic (*7*) picoplanktonic flora has led to a new paradigm for biogeochemical cycling in marine surface wa-

E. J. Carpenter, Marine Sciences Research Center, State University of New York, Stony Brook, NY 11794–5000. K. Romans, SEA Education Association, Woods Hole, MA 02543.

*To whom correspondence should be addressed.